Journal of Innovative Optical Health Sciences
Vol. 7, No. 2 (2014) 1350038 (11 pages)

DOI: 10.1142/S1793545813500387

World Scientific
www.worldscientific.com

Real-time *in situ* detection and quantification of bacteria in the Arctic environment

Linda Powers*,§, Walther R. Ellis Jr.†
and Christopher R. Lloyd‡
*Department of Electrical and Computer Engineering
Department of Biomedical Engineering
University of Arizona, Tucson, AZ 85721

†Department of Biomedical Engineering
University of Arizona, Tucson, AZ 85721

‡MicroBioSystems of Arizona, 1665 E 18th St.
Suite 204, Tucson, AZ 85719
§lsp@ece.arizona.edu

Received 18 July 2013
Accepted 19 August 2013
Published 26 September 2013

At present, there are no methods that determine the total microbial load on an abiotic substrate in real time. The utility of such a capability ranges from sterilization and medical diagnostics to the search for new microorganisms in the environment and study of their ecological niches. We report the development of a hand-held, fluorescence detection device and demonstrate its applicability to the field detection of Arctic bacteria. This technology is based on the early pioneering work of Britton Chance which elucidated the intrinsic fluorescence of a number of metabolites and protein cofactors in cells, including reduced pyridine nucleotides, cytochromes and flavins. A PDA controls the device (fluorescence excitation and data collection) and processes the multiwavelength signals to yield bacterial cell counts, including estimates of live cells, dead cells and endospores. Unlike existing methods for cell counting, this method requires no sample contact or addition of reagents. The use of this technology is demonstrated with *in situ* measurements of two sub-glacial microbial communities at sites in Palander and colonized surface rocks in the Bockfjord Volcanic Complex during AMASE 2008 (Arctic Mars Analog Svalbard Expedition). The total bacterial load on the interrogated sample surfaces ranged from < 20 cells/cm^2 to $> 10^9$ cells/cm^2.

Keywords: Intrinsic fluorescence; microbial sensor; optical detection; amplitude modulation; Svalbard Archipelago.

1. Introduction

There is considerable interest in determination of the viability and location of microbes in the environment (and their ecological niches). Medical applications include sterilization and antibiotic efficacy as well as the discovery of new antibiotics and the development of diagnostics. We report the development of a hand-held, fluorescence detection device and demonstrate its applicability to the field detection of Arctic bacteria. This technology is based on the early pioneering work of Britton Chance which elucidated the intrinsic fluorescence of a number of metabolites and protein cofactors in cells, including reduced pyridine nucleotides, cytochromes and flavins. While most of his applications were biomedical, we have extended these to include microorganisms that populate harsh environments. These include polar regions of the earth, high deserts, sub-terrestrial zones (e.g., caverns) and deep undersea vents, which are of particular interest with regard to determining the physic-chemical limits of known life forms and possibly extrapolating these to the search for life on other planetary bodies. In this context, searching for new microbial forms of life has proven to be tedious, requiring blind sampling and transport of samples to laboratories for subsequent characterization by biochemical analyses (DNA, lipids, etc.).

At present, the determination[1] of total microbial load is qualitative and largely relegated to the laboratory, with the main alternatives including classical plate counts, direct microscopic examination of concentrated suspensions ($>10^7$ cells/ml), PCR amplification of a range of genes, simple enzyme-based assays,[2] and fluorescence measurements using DNA-intercalating dyes (e.g., using epifluorescence microscopy or flow cytometry). A significant problem with any method that relies on laboratory outgrowth of an environmental sample is the viable-but-not-culturable phenomenon,[3] which typically leads to significant underestimates of the numbers of cells and diversities of cells in real-world samples. A cell-counting method that is broadly applicable to microorganisms, and applicable to a variety of sampling problems (water, ice, soil, rock), would be highly useful in guiding sampling work in the field.

A variety of optical techniques have been applied to the detection and quantification of microbes, particularly involving scattering or spectroscopy. Simple light scattering (culture turbidity) in the visible region is commonly used to determine the concentration of cells in liquid suspension. Advances in instrumentation and data processing have enabled IR and Raman[4–7] measurements on microbial colonies, and commercial instruments (e.g., River Diagnostics and Brucker) are available for specific microbial identification based upon the comparison of "fingerprint" regions in spectra with reference spectra in a database. However, prior outgrowth on manufacturer-specified media is required. Current commercial instruments, including field-portable ones (e.g., Ocean Optics systems), are suitable for obtaining spectra of millimeter-sized colonies of cells that are visible to the eye, but not low numbers of cells. The addition of a microscope to the optical path of an instrument (as in a Raman microspectrometer) solves this problem, but renders the equipment even more difficult to use in the field.

Fluorescence methods provide the most sensitive optical detection of biomolecules. High fluorescence sensitivity, coupled with a short-collection-time requirement, and the ability to monitor large areas/volumes continuously are very attractive for the *in situ* investigation of microbes in the environment. We developed a multiwavelength fluorescence instrument to distinguish live bacterial cells, dead cells and endospores, based on the intrinsic fluorescence[8] of a number of metabolites and protein cofactors.[9–14] Importantly, our approach does not rely on 260–280 nm excitation because this excites aromatic amino acids, purines and pyrimidines; these are ubiquitous in real-world samples. More than 50 years ago, it was noted in the early work of Britton Chance[15,16] and others[17,18] that the fluorescence due to NAD[P]H decays upon cell death as the oxidized forms (NAD[P]+) accumulate. Pyridine nucleotide fluorescence occurs at Ex 365 nm/Em 440 nm, with small contributions from other fluorophores. Bacterial sporulation is accompanied by the production of a distinctive, fluorescent calcium dipicolinate complex that is densely packed in the endospore; this fluorescence (Ex 635 nm/Em 770 nm) disappears as the compound is expelled when the spores germinate.[14] Nonviable cells, those not respiring but maintaining some level of cellular integrity, exhibit fluorescence (Ex 590 nm/Em 675 nm) from flavins, cytochromes and apo forms of porphyrins. Other microbial components also fluoresce: bacteriochlorophylls, phycocyanins and phycoerythrins, siderophores such as pyroverdins and deferrioxamines, and some B-vitamins.[19]

We report field measurements of microbial communities at sites in the Svalbard Archipelago, Norway, during AMASE 2008 (Arctic Mars Analog Svalbard Expedition, http://amase.ciw.edu/) using a prototype, high-sensitivity device to detect intrinsic bacterial fluorescence. This methodology was specifically tailored for the determination of total cell counts, apportioned among live cells, dead cells and endospores, in colonies *in situ* (i.e., without sample contact or the use of added reagents such as fluorescent dyes).

2. Materials and Methods

2.1. *Sample handling and preparation*

Two *in situ* measurements were made in different sections of the Palander ice cap. Site 1 was at the base of the ice cap, in a gully having about 10 cm of granular snow over about 2.5 cm of solid ice. Site 2 was near the top of the ice cap, on a 15–20° slope, and consisted of 15 cm of granular snow with about 32 cm of ice on top of rock (approximate position in UTM, 061457 easting and 884409 northing). The sites were separated by approximately 500 m. For each site, measurements of ice and snow were taken about every 1 cm using a small sterile shovel to remove the top layer until a rocky underlayer was reached. During the measurements, no physical contact was made with sample.

After the *in situ* measurements at Sites 1 and 2, described below, a rock from each site was collected by aseptic methods and stored in a sterile container. After returning to our laboratory in the US, the surfaces of both rocks were scraped, the residues suspended in pH 7.2 phosphate-buffered saline (PBS) medium, and then streaked onto a variety of media reported for outgrowth of Arctic microbes[20–23] at 4°C under illumination. After ca. 10 weeks, plates were surveyed, and individual colonies were lifted and replated to obtain pure isolates (4°C, under illumination). Scrapings from both rocks were additionally stained (malachite green/safranin) and examined by light microscopy, which revealed no endospores.

Three colonies from the Site 1 rock were grown out in R2A medium (2°C) (dehydrated broth purchased from Teknova, http://www.teknova.com), centrifuged, and their genomic DNAs were extracted and purified using a Qiagen QIAprep DNA kit. We used a primer pair V3 F,R[24,25] synthesized by Bioneer, and amplified a region of 16 S ribosomal RNA genes using Promega Go-Taq PCR Core System II reagents and a Bio-Rad MyiQ real-time PCR detection system. The same reagents were used to scale up the PCR amplifications (minus SybrGreen I dye) (PCR thermal cycler program as follows: 30 s at 95°C, then 35 cycles (30 s at 95°C, 60 s at 60°C, 45 s at 72°C) for sequencing of the V3 amplicons (204 bp). PCR-amplified DNAs were gel-purified using Invitrogen TBE gels, and then submitted to the Arizona Research Laboratory Genomic Analysis and Technology Core facility. Both strands of each amplicon were sequenced, using sequencing primers derived from the PCR primers noted above. The DNA sequences were then queried (January 2012), using the BLAST software tool (www.ncbi.nlm.nih.gov), in homology searches against 16 S ribosomal RNA gene sequences in the GenBank database. The searches identified the isolates as *Cryobacterium psychrophilum* (99% sequence similarity to the DSM 4854 strain), and two *Pseudomonas* spp. (100% sequence similarities). Site 2 outgrowth on Z-agar[26] (produced monodispersed off-white, rod-shaped cells at 4°C. A search identified the bacterium recovered from Site 2 as a *Bacillus* sp. (100% sequence similarity).

Rocks were also collected around Bockfjord Volcanic Complex, Svalbard, and were optically interrogated within 12 h post-collection. These samples were collected and transported in sterile bags. Some of these were small enough to be transported to our laboratory where they were autoclaved, scraped and/or cleaved to expose previously unexposed surfaces, as described in the instrument calibration section and measured again after wetting with distilled water. Others were too large for transport, so we measured several points of interest (especially endoliths and weathered sections) on each rock, then cleaved off sections of the rock to allow measurement of portions underneath where we had made surface measurements, but which were not exposed to the elements. Some of the collected rock samples showed a very large increase in the 440 nm fluorescence after autoclaving. A cursory examination suggested this was due to the production of fluorescent organic byproducts from the heat. For each of these, a section was then scraped to expose a previously unexposed surface, or an unexposed inside section was produced by cleaving the rock. These latter values were used in lieu of the autoclaved values as a background measurement.

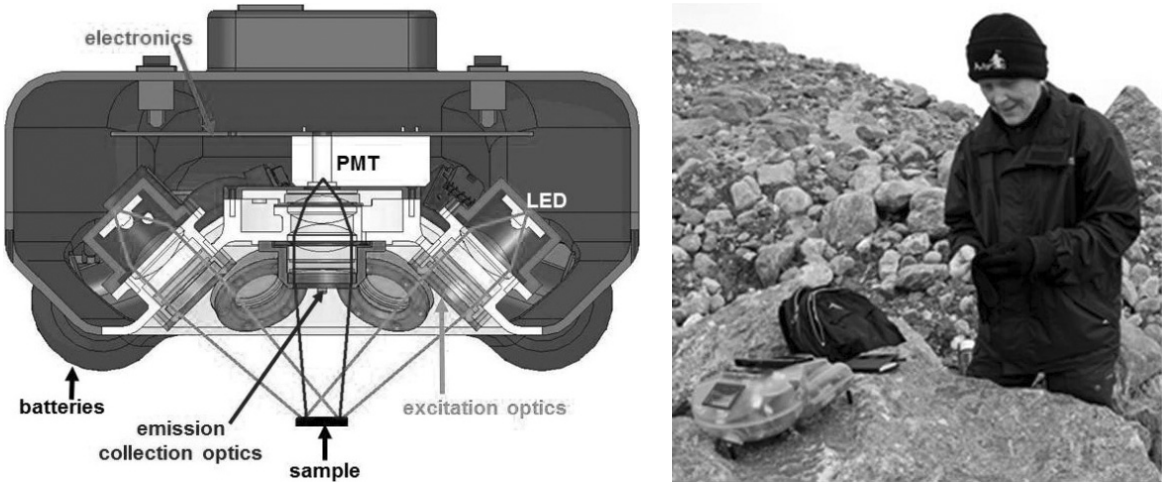

Fig. 1. Cut-away view [left] and picture [right, lower left corner] of the intrinsic fluorescence instrument used in these studies.

2.2. *Multiwavelength intrinsic fluorescence instrument*

Descriptions of earlier intrinsic fluorescence detectors for cell detection and their application to the determination of total microbial load are given by Powers and collaborators.[9–14,27] The instrument used in this study was specifically designed for the measurement of surfaces in the field, and is diagrammatically shown in Fig. 1. Three light emitting diode (LED) sources having an emission around the designated wavelength of ∼10 nm at full-width at half-maximum (FWHM) are used for excitation (Ex) of the desired fluorescence emission (Em) from the sample. These LEDs are filtered using interference filters to remove the long-wavelength tail typical of these sources, and an excitation-rejection interference filter is used in front of the photomultiplier tube (PMT) detector. Figure 2 shows the optical outputs of the LEDs, the respective emission (fluorescence) signatures for viable bacterial cells, nonviable cells and endospores, and the cut-off of the Rugate excitation-rejection filter in front of the PMT.

The LEDs are also pulsed at different frequencies.[27] Since the resultant fluorescence has the same frequency modulation as its excitation, all three fluorescence emissions can be observed simultaneously with a single PMT (with an interference filter to reject the excitation light) if they are modulated at unique frequencies. This also significantly lowers the cost (one PMT is needed, instead of one for each emission channel). The individual fluorescence contributions can subsequently be separated by Fourier transformation. This approach significantly narrows the noise bandwidth, which dramatically enhances the signal-to-noise ratio, and thus makes the instrument useful in detecting microbial populations that vary by orders of magnitude. The frequency-modulated fluorescence signals and their respective Fourier transforms are reported on a general user interface, together with values of the integrated signals under the Fourier transform peaks. An algorithm is then used to estimate the total bacterial load within an order of magnitude, and also the relative amounts of viable cells, nonviable cells and endospores, based on calibrations of the instrument with a variety of bacteria.[28]

2.3. *Instrument calibration*

The multiwavelength fluorescence instrument was calibrated using laboratory-prepared samples (washed 4 times with PBS, to remove fluorescent components in LB medium) of *Bacillus thuringiensis* (ATCC 10792) and *Escherichia coli* (ATCC 15222) containing known amounts of viable cells, nonviable cells and endospores before travel to Svalbard. Table 1 shows the contributions of viable cells, nonviable cells and endospores to each of the Ex/Em pairs we used, using equal amounts of the three components.[12] An Invitrogen LIVE/DEAD

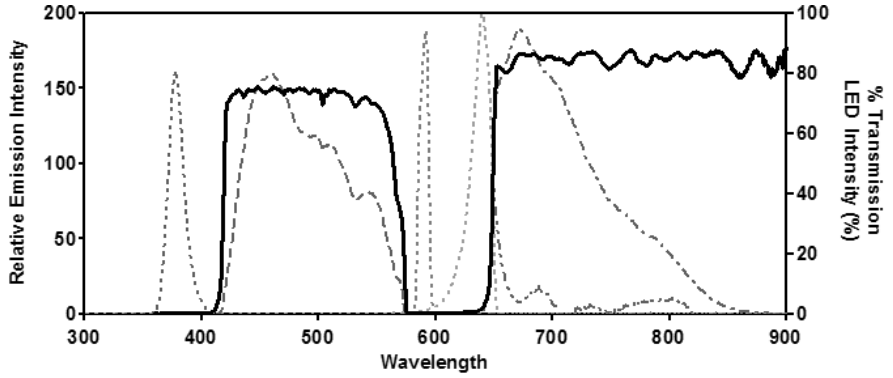

(a)

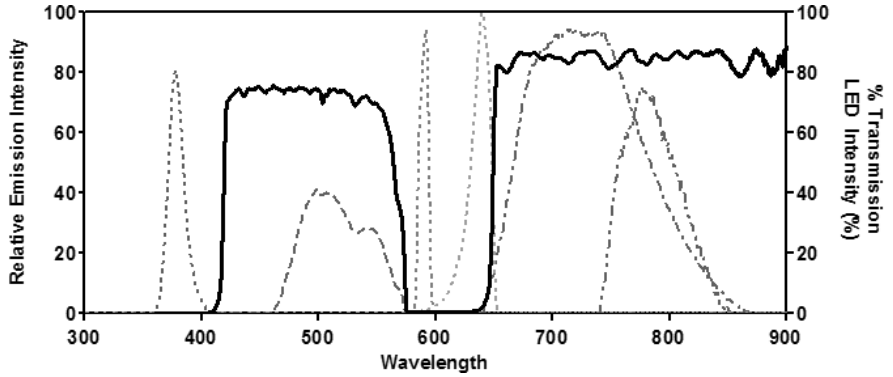

(b)

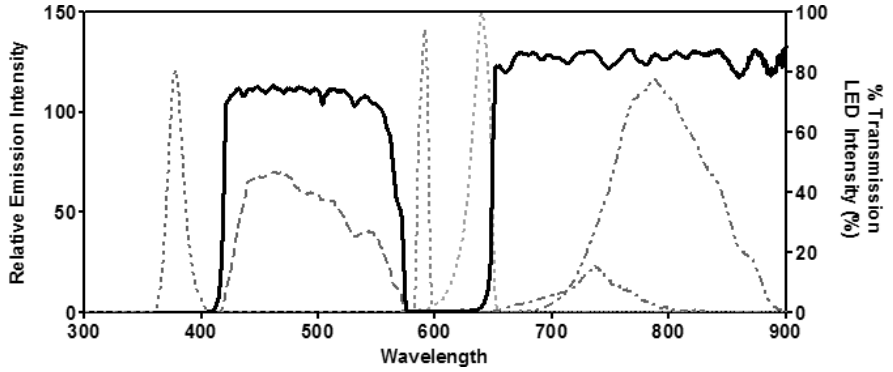

(c)

Fig. 2. Spectra for the LED sources, fluorescence bands, and the cut-off of the excitation rejection filter on the PMT detector for live cells (panel a), dead cells (panel b) and endospores (panel c). The filter characteristics are shown as the solid line and % transmission on the right axis. The three excitation bands are noted as dotted lines. The fluorescence emissions are as follows: 365 nm excitation, dashed line; 590 nm excitation, dashed-dot line; and 635 nm excitation, dashed-dot-dot line.

*Bac*Light cell viability kit was used, together with direct cell counting (Nikon fluorescence microscope), to estimate the live/dead fractions in cell suspensions, and parallel (unstained) samples were interrogated with our instrument for calibration purposes. Although the instrument had been temperature-calibrated to compare data collected in the field with those collected in the laboratory, optically clear plastic-laminated samples of *B. thuringiensis* endospores were used to verify the instrument calibration immediately before and after measurements in the field.

For post-expedition calibration using Svalbard-collected bacteria, we chose a Site 1-derived bacterium,

Table 1. Fluorescence channels: Bacterial cell contributions.[11,12]

Excitation/emission	Contributions
365 nm/440 nm	0.7 live cells + 0.15 dead cells + 0.15 endospores
590 nm/675 nm	0.5 live cells + 0.5 dead cells
635 nm/770 nm	0.5 dead cells + 0.5 endospores

Note: Assuming equal numbers of live cells, dead cells, and endospores in the sample.

Pseudomonas sp. Once growth was confluent, cell samples were scraped off an agar plate, suspended in 4°C PBS, lightly vortexed, and then centrifuged (3000 × g, 10 min). Pelleted cells were then resuspended in PBS, centrifuged and resuspended in PBS three additional times to wash out extracellular fluorophores. Cell densities of the resulting bacterial suspensions were determined by optical microscopy after staining with acridine orange, using a Petroff-Hausser counting chamber, and known dilutions of a parallel, unstained bacterial stock were then prepared for instrument calibration.

Approximately, 200 μL of pure water was added to the rock surface and the fluorescence was measured. This was repeated for PBS added to the rock surface. This quantity wetted the rock surface area measured by the instrument (ca. 1 cm^2), resembling the conditions of the *in situ* Svalbard measurements.

The Site 2 rock was treated similarly, using the Site 1-derived pseudomonad. The dilution range measured was generally from ca. 10^4–10^7 cells/mL (or approximately 10^3–10^6 total cells in the measured $\sim$1 cm^2 area). These measurements were

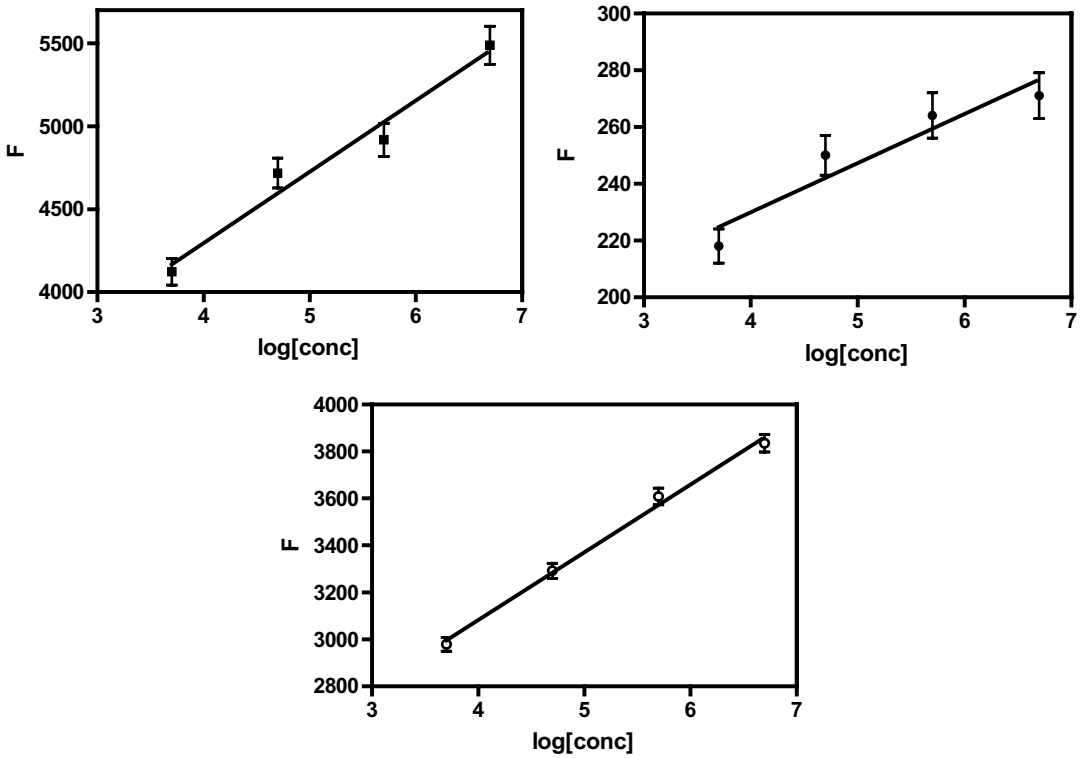

Fig. 3. Calibration curves using *Pseudomonas* sp. cells isolated from the outgrowth of the sample from Palander Site 1. F is the measured fluorescence in relative units and the surface concentration is in cells/cm^2. For the 635 nm excitation/770 nm emission pair [top left], $F = 429.7$ log[conc] + 2577.1 with $R^2 = 0.97$. For the 590 nm excitation/675 nm emission pair [top right], $F = 17.2$ log [conc] + 162.0 with $R^2 = 0.89$. For 365 nm excitation/440 nm emission pair [bottom], $F = 288.4$ log[conc] + 1929.4 with $R^2 = 0.995$. R^2 is the square of the Pearson product moment correlation coefficient.

used to produce plots for each excitation band that subsequently were used to estimate the microbial concentrations measured *in situ* (see Fig. 3). This calibration, with cells of Svalbard origin on Svalbard collected rocks, was very similar to that done before the expedition in our laboratory with *B. thuringiensis* (ATCC 10792) and *E. coli* (ATCC 15222). As discussed below, the fluorescence contribution [Ex 630 nm/Em 770 nm] indicative of both nonviable cells and endospores, was negligible; hence, no additional post-expedition calibration using endospores produced from a Svalbard-collected *Bacillus* sp. was carried out.

The fluorescence contributions of live cells, dead cells and endospores to each of the emission channels were thus determined by calibrating the instrument using two reference strains and the *Bac*Light viability kit (differential staining using two DNA-binding fluorophores), and a bacterium isolated from a Svalbard environmental sample. The calibrations agreed within experimental error.

Four partial 16S rRNA gene sequences have been deposited in the GenBank database, one for each bacterium cultured and noted previously, with the following accession numbers: JQ688002, JQ688003, JQ688004 and JQ688005.

3. Results

3.1. *Calibrations*

Calibration data using isolated *Pseudomonas* sp. cells in PBS on the collected Site 1 rock surface are shown in Fig. 3. These results were used to estimate the respective cell concentrations on rocks *in situ* (see Table 2) and on rocks collected around Bockfjord Volcanic Complex (see Table 3). Since pseudomonads do not form endospores, the Ex 635 nm/Em 770 nm graph of Fig. 3 (top, left) is entirely due to dead cells. This is due to the fact that the contributors to the emission observed for Ex 635 nm/Em 770 nm are dead and sporulated cells (see Table 1).

3.2. *Field measurements*

Referring to data in Fig. 3 (top left panel and legend), readings below 2577 for this channel indicate less than one cell in the spot being illuminated. Hence, the concentrations associated with the Ex 63 nm/Em 770 nm values of Table 2 are essentially zero. This means that the concentration of endospores and nonviable cells is negligible at the two Palander sites. This also simplifies the solutions to the equations in Table 1, since the Ex 365 nm/Em 440 nm and Ex 590 nm/Em 670 nm excitation/emission pairs now measure only live cells.

Table 2 shows the results of the *in situ* Palander measurements, with direct comparison with the calibration curves of Fig. 3 for determination of the concentration for each excitation/emission pair. The concentration of live cells for each measurement is a weighted average based on the R^2 values of the Ex 590 nm/Em 670 nm and Ex 365 nm/Em 440 nm excitation pairs data of Fig. 3. At Site 1, a concentration of $2 \times 10^4 \pm 6 \times 10^2$ live cells/cm^2 was found with no endospores or dead cells (within the error). Site 2 was similar, having essentially no endospores or dead cells, but it had a larger

Table 2. Palander rock surface fluorescence measurements[a] and derived cell counts.

	Em data (error)			Cell concentration (cells/cm^2)				
	Ex			Ex				
Rock	635	590	365	635	590	365	Endospores + Nonviable cells (cells/cm^2)	Live cells (cells/cm^2)
Site 1	2277 (24)	231 (10)	3146 (35)	0	1.1×10^4	1.7×10^4	0	1.6×10^4
	2541 (34)	239 (15)	3160 (44)	0	3.4×10^4	1.9×10^4	0	2.2×10^4
Site 2	2665 (37)	281 (9)	3937 (69)	1.6	8.3×10^6	9.4×10^6	3.2	8.8×10^6

[a]Fluorescence data (Em value for each of the 635, 590, 365 nm excitation channels) expressed in terms of relative fluorescence units. Error is the standard deviation in the measurement. See Table 1 for contributions of live/dead/sporulated cells to each channel.

Table 3. Results for rocks collected around the Bockfjord volcanic complex.

Rock	Em data after subtraction of background[a] Ex 635	Ex 590	Ex 365	Concentration from calibration[b] (cells/cm^2) Ex 635	Ex 590	Ex 365	Endospores + Nonviable (cells/cm^2)	Live cells (cells/cm^2)
1	310	0	228	5.6	0	5.3	5.6	0
2	1628	215	1069	8.2×10^3	1.3×10^3	2.6×10^3	8.2×10^3	0
3	1248	138	830	1.0×10^3	1.0×10^2	4.5×10^2	1.0×10^3	0
4	52	0	373	1.3	0	1.6×10^1	1.3	1.4×10^1
5	656	91	554	3.8×10^1	2.1×10^1	5.9×10^1	3.8×10^1	2.1×10^1
6	0	19	286	1.0	1.9	8.2	1.0	7.2
7	332	88	237	6.3	1.9×10^1	5.7	6.3	0
7 back	371	56	463	7.8	6.6	3.0×10^1	7.8	2.2×10^1
8	0	51	60	1.0	5.6	1.6	1.0	0
8 back	41	27	0	1.3	2.4	1.0	1.3	0
9	0	21	65	1.0	2.0	1.6	1.0	0
9 back	669	109	480	4.1×10^1	3.8×10^1	3.4×10^1	4.1×10^1	0
10	1443	249	1074	2.9×10^3	4.2×10^3	2.7×10^3	2.9×10^3	0
10 back	367	123	0	7.6	6.2×10^1	1.0	7.6	0
11	50	243	1203	1.3	3.4×10^3	6.9×10^3	1.3	6.9×10^3
11 back	822	292	1380	9.5×10^1	1.8×10^4	2.6×10^4	9.5×10^1	2.6×10^4
12	0	35	0	1.0	3.3	1.	1.0	0
12 back	0	5	0	1.0	1.2	1.0	1.0	0
13	3115	610	2810	3.1×10^7	7.7×10^8	9.5×10^8	3.1×10^7	9.2×10^8
13 back	3710	604	2932	8.3×10^8	6.2×10^8	2.3×10^9	8.3×10^8	1.5×10^9
14	3092	345	255	2.7×10^7	1.0×10^5	6.5	2.7×10^7	0
15	0	25	317	0	2.3	1.0×10^1	0	1.0×10^1
16 endoliths (inside)	10474	1372	10982	$> 10^9$	$> 10^9$	$> 10^9$	$> 10^9$	$> 10^9$
16 weathered (inside)	5370	798	5170	$> 10^9$	$> 10^9$	$> 10^9$	$> 10^9$	$> 10^9$
16 side 2 (exposed)	1557	175	0	5.5×10^3	3.5×10^2	0	5.5×10^3	0

[a]Values are relative fluorescence units.
[b]See Fig. 3 for representative data.

bacterial concentration of $(7.60 \pm 0.08) \times 10^6$ live cells/cm^2. Essentially no bacterial life (within the error) was detected in ice cores or the ice and snow above the ice/rock interface using this instrumentation, which interrogates $\sim$1cm^2 per measurement. This does not necessarily mean that none exist, but that the number of cells per cm^2 is below our detection limit for this area. Alternatively, microbial life in the Palender ice might exist in "oases", often associated with dust,[14] that we did not encounter in sampling.

From the calibration curves shown in Fig. 3, the detection limit for this instrument was determined by extrapolation to be approximately 20 cells on the Site 1 rock surface of approximately 1 cm^2. Since the autoclaved/scraped/cleaved rocks from both Palander sites with only pure water on them (or PBS solution) show fluorescence values that are within the error of the respective y-intercepts of the calibration curves of Fig. 1, the bacterial fluorescence is independent of the rock fluorescence. Hence, we can use these calibrations to determine the bacterial loads of other rock surfaces provided we subtract the wet autoclaved/scraped/cleaved value for each rock from the data measured on site and use the slope of the calibration plot to estimate the concentration from this difference.

In the sole case where a whole rock could be extracted from Palander Site 1 and kept in a sterile plastic bag, our measurements made in the Svalbard laboratory up to 24 h later agree with those made in the field (within experimental error). At Site 2, a portion of the rock measured *in situ* had to be separated from a much larger boulder, and some of the live cell population may have been killed.

3.3. *Collected rock samples from the Bockfjord volcanic complex*

These were identified by Dr Marc Fries (AMASE member) as marble with fractures, peridotite xenolith with some adhering basalt, low-grade metasediment with some amphibolite, metasediment, red bed material Devonian sediment, vesicular basalt, basalt with carbonate weathering rind, cemented breccia, cement is carbonate with angular basalt fragments, slightly supporting matrix basalt with weathering rind of carbonate and iron oxide, basalt with carbonate, basalt weathered pebbles, remelted gneiss (found as float), peridotite xenolith with a carbonate weathering rind, and lightly metamorphosed marble. A total of 16 rock samples were analyzed on site (some on two sides) for total bacterial load and the results are shown in Table 3. Of these 25 measurements, 19 showed 0–10^1 live bacterial cells/cm^2, 1 showed $\sim 10^3$/cm^2, 1 showed 10^4/cm^2 and 4 showed $>10^8$/cm^2. The measured fluorescence is not linear in concentration for concentrations >ca. 10^9 cells/cm^2 and these cell counts should be considered as lower limits.

4. Discussion

Our measurements are in agreement with conclusions of other investigations that the subglacial population of bacteria is significantly larger than those of ice cores from large ice sheets. Microbial communities exist at glacier beds and in subglacial sediments in both the Northern[22,24,29,30] and Southern Hemispheres.[23,31] We have shown that these communities can be measured *in situ* with our multiwavelength intrinsic fluorescence technology and find 10^4 cells/cm^2 and 10^7 cells/cm^2, respectively, for two communities at the rock/glacier interface at the Palander ice cap in the Svalbard archipelago. These are comparable to an estimate of 10^5 cells/cm^2 from the data of Kaštovská *et al.*[20] for two polythermal glaciers, Werenskioldbreen and Torellbreen, southwest Spitsbergen, Svalbard, and 10^4 cells/cm^2 for the data of Srinivas *et al.*[32] from Kongsfjorden and Ny-Alesund. They are also comparable to those estimated from two glaciers in the southern hemisphere.[33] We did not observe fluorescence signals or staining that are characteristic of microbial endospores,[9–14] despite our isolation of a *Bacillus* strain from the Svalbard Site 2 sample. In this context, it is important to note that the rocks taken from both Palander sites were covered with a thin layer of meltwater at the time of optical interrogation and sample collection — this could have been a significant reason why the cells appeared to be in a vegetative state rather than sporulated.

Our experimental results show a large variance in cell density, approximately nine orders of magnitude in the Bockfjord rock samples. This has clear implications for environmental microbiologists interested in diversity and ecology, since sample collection and processing are both time-consuming and expensive. Multiwavelength fluorescence, collected on site with a portable instrument, could be used to locate highly populated sites and thus guide sampling efforts, subject to some caveats. First, a high abiotic surface fluorescence would necessarily make the instrument detection limit higher. Second, this instrument is designed to collect fluorescence from a surface, not a liquid sample. We have designed and tested a fluorescence collector for bacteria in a water column, and will report this elsewhere. Third, while *in situ* measurements likely reflect a distribution of metabolic states, it is not clear that this distribution for bacteria used for calibrations [grown to mid-log phase, washed, and resuspended in PBS] accurately mimics that of environmental samples. A skewed distribution of metabolic states of the bacterial populations on samples being measured, or those used for calibration, will lead to an under- or overestimation of the live cell concentration by factors <3.

Other microbial fluorophores are not observed with this instrument, due to its optical design. Additional intrinsic fluorophores and pigments may absorb (due to energy transfer) one or more of the fluorescence emissions measured by this instrument, causing measurements to be less than expected for the affected channels. *Pseudomonas* spp., for example, produce siderophores (pyochelins). Their fluorescence would appear in the UV (Ex 365 nm/Em 440 nm) region, which would increase the viable cell count somewhat if this channel were used alone. None of the three emission channels are based on just one fluorescence signature, however. This feature corrects for the appearance of unwanted fluorescence signatures that could seriously mislead the user, and is incorporated into the signal processing software. In summary, the three independent equations of Table 1 contain three unknowns, which are related to each other by three independent measurements.

Using a commercial spectrofluorimeter outfitted with a fiber optic cable, it is possible to obtain multiwavelength fluorescence data from surfaces. However, the optical collection efficiency is not currently sufficient to obtain good-quality data from modest numbers of cells (e.g., $10^4/\text{cm}^2$) on an abiotic surface. Furthermore, such instruments cannot be used to acquire data in the presence of sunlight or room light; our instrument circumvents this problem through the use of PMT measurements before and after each excitation pulse. The instrument used for this work contained batteries sufficient for about 5 h of operation in the Arctic temperatures, weighed 1.3 kg, and easily fits into a small backpack (Fig. 2, right).

5. Conclusions

The results presented in this study demonstrate that a handheld microbe sensor that requires no sample preparation or added reagents is feasible. Variations of this technology may also find use on remotely operated vehicles in surveys of harsh environments and microbial water quality assessments. While this instrument was developed and used to study bacteria, we have shown that other microorganisms of environmental interest (e.g., archaea, fungi) can be studied using similar equipment and data analysis algorithms. A refinement of our design should result in a weight below 0.5 kg and greater portability due to smaller volume. Finally, it is important to note that there is likely an additional analytical value in determining fluorescence lifetime information as well as intensities. This will require high-speed data acquisition, with careful attention to LED and PMT on-off timing, and will be the focus of a future report.

In Memory of Britton Chance

The truly wonderful thing about Brit, and maybe the most significant contribution he made to society, was his blindness to gender, race, or origin. He simply did not care. If you had interest and talent, he was there to help. He supported women, minorities, and foreigners when it was not a fashionable [or government mandated] thing to do. Look around you at the contributions that have been made by those he mentored and the example he set for all of us to follow! This is truly awesome and inspiring.

Acknowledgments

This work was supported by AMASE under the NASA ASTEP program (A. Steele PI), the Thomas R. Brown Foundation, and the University of Arizona. The authors thank Hans Amundsen, Pam Conrad, Andrew Duncan, Miriam Eaton, Marc Fries, Michael Garrett, Steven Squyres, Andrew Steele and Lois Wardell for support during various phases of this work.

References

1. N. S. Hobson, I. Tothill, A. P. F. Turner, "Microbial detection," *Biosens. Bioelectron* **11**, 455–477 (1996).
2. M. Manafi, W. Kneifel, S. Bascomb, "Fluorogenic and chromogenic substrates used in bacterial diagnosis," *Microbiol. Rev.* **1991**, 335–348 (1991).
3. J. Oliver, "Recent findings on the viable but nonculturable state in pathogenic bacteria," *FEMS Microbiol. Rev.* **34**, 415–425 (2010).
4. N. Tarcea, M. Harz, P. Rösch, T. Frosch, M. Schmitt, H. Thiele, R. Hochleitner, J. Popp, "UV Raman spectroscopy — a technique for biological and mineralogical *in-situ* planetary studies," *Spectrochim. Acta* **68A**, 1029–1035 (2007).
5. M. Krause, P. Rösch, B. Radt, J. Popp, "Localizing and identifying living bacteria in an abiotic environment by a combination of Raman and fluorescence microscopy," *Anal. Chem.* **80**, 8568–8575 (2008).
6. M. Harz, P. Rösch, J. Popp, "Vibrational spectroscopy — a powerful tool for the rapid identification of microbial cells at the single-cell level," *Cytometry* **75A**, 104–113 (2009).
7. J. J. Ojeda, M. E. Romero-González, S. A. Banwart, "Analysis of bacteria on steel surfaces using reflectance micro-Fourier transform infrared spectroscopy," *Anal. Chem.* **81**, 6467–6473 (2009).
8. M. S. Ammor, "Recent advances in the use of intrinsic fluorescence for bacterial identification and characterization," *J. Fluorescence* **17**, 455–459 (2007).
9. L. Powers, "Method and apparatus for sensing the presence of microbes," U.S. Patent 5,760, 406 (1998).
10. L. Powers, "Method and apparatus for sensing the presence of microbes," U.S. Patent 5,968, 766 (1999).
11. C. Estes, A. Duncan, B. Wade, C. Lloyd, W. Ellis Jr., L. Powers, "Reagentless detection of microorganisms by intrinsic fluorescence," *Biosens. Bioelectron* **18**, 511–519 (2003).
12. L. Powers, C. R. Lloyd, "Method and apparatus for detecting the presence of microbes and determining their physiological status," U.S. Patent 6,750, 006 (2004).

13. L. Powers, C. R. Lloyd, "Method and apparatus for detecting and imaging the presence of biological materials," U.S. Patent 7,186, 990 B2 (2007a).
14. L. Powers, C. R. Lloyd, "Method for detecting the presence of dormant cryptobiotic microorganisms," U.S. Patent 7,211, 377 B1 (2007b).
15. B. Chance, *The Harvey Lectures, Series 49, 1953–1954*, Academic Press, NY, pp. 145–175 (1955).
16. B. Chance, B. Theorell, "Localization and kinetics of reduced pyridine nucleotide in living cells by microfluorimetry," *J. Biol. Chem.* **2234**, 3044–3050 (1959).
17. L. Duysens, J. Amesz, "Fluorescence spectrophotometry of reduced phosphopyridine nucleotide in intact cells in the near-ultraviolet and visible regions," *Biochim. Biophys. Acta* **24**, 19–26 (1957).
18. A. Alimova, A. Katz, H. E. Savage, M. Shah, G. Minko, D. V. Will, R. B. Rosen, S. A. McCormick, R. R. Alfano, "Native fluorescence and excitation spectroscopic changes in *Bacillus subtilis* and *Staphylococcus aureus* bacteria subjected to conditions of starvation," *Appl. Opt.* **42**, 4080–4087 (2003).
19. J. Lackowicz, *Topics in Fluorescence Spectroscopy*, Vol. 3, Plenum Press, New York (1991).
20. K. Kaštovská, J. Elster, M. Stibal, H. Šantrucková, "Microbial assemblages in soil microbial succession after glacial retreat in Svalbard (high Arctic)," *Microb. Ecol.* **50**, 396–407 (2005).
21. S. M. Cheng, J. M. Foght, "Cultivation-independent and -dependent characterization of bacteria resident beneath John Evans glacier," *FEMS Microbiol. Ecol.* **59**, 318–330 (2007).
22. K. Kaštovská, M. Stibal, M. Šabacká, B. Cerná, H. Šantrucková, J. Elster, "Microbial community structure and ecology of subglacial sediments in two polythermal Svalbard glaciers characterized by epifluorescence microscopy and PLFA," *Polar Biol.* **30**, 277–287 (2007).
23. B. Lanoil, M. Skidmore, J. C. Priscu, S. Han, W. Foo, S. W. Vogel, S. Tulaczyk, H. Engelhardt, "Bacteria beneath the West Antarctic Ice Sheet," *Environ. Microbiol.* **11**, 609–615 (2009).
24. J. L. Wadham, S. Bottrell, M. Tranter, R. Raiswell, "Stable isotope evidence for microbial sulphate reduction at the bed of a polythermal high Arctic glacier," *Earth Planet. Sci. Lett.* **219**, 341–355 (2004).
25. S. Chakravorty, D. Helb, M. Burday, N. Connell, D. Alland, "A detailed analysis of 16S ribosomal RNA gene segments for the diagnosis of pathogenic bacteria," *J. Microbiol. Methods* **69**, 330–339 (2007).
26. R. Atlas, *Handbook of Media for Environmental Microbiology*, 2nd edition, p. 634, Taylor & Francis, Boca Raton, FL (2005).
27. L. Powers, C. R. Lloyd, "Method and apparatus for detecting the presence of microbes with frequency modulated multiwavelength intrinsic fluorescence," U.S. Patent 7,824, 883 (2010).
28. B. R. Copeland, M. Chen, B. D. Wade, L. S. Powers, "A noise-driven strategy for background estimation and event detection in data streams," *Signal Process.* **86**, 3739–3751 (2006).
29. M. Sharp, J. Parkes, B. Craig, I. J. Fairchild, H. Lamb, M. Tranter, "Widespread bacterial populations at glacier beds and their relationship to rock weathering and carbon cycling," *Geology* **27**, 107–110 (1999).
30. M. L. Skidmore, J. Foght, M. J. Sharp, "Microbial life beneath a high Arctic glacier," *Appl. Environ. Microbiol.* **66**, 3214–3220 (2000).
31. J. A. Mikucki, A. Pearson, D. T. Johnston, A. V. Turchyn, J. Farquhar, D. P. Schrag, A. D. Anbar, J. C. Priscu, P. A. Lee, "A contemporary microbially maintained subglacial ferrous 'ocean'," *Science* **324**, 397–400 (2009).
32. T. N. Srinivas, S. S. N. Rao, P. V. V. Reddy, M. S. Pratibha, B. Sailaja, B. Kavya, K. K. Hara, Z. Begum, S. M. Singh, S. Shivaji, "Bacterial diversity and bioprospecting for cold-active lipases, amylases and proteases, from culturable bacteria of Kongsfjorden and Ny-Alesund, Svalbard. Arctic," *Curr. Microbiol.* **59**, 537–547 (2009).
33. J. Foght, J. Aislabie, S. Turner, C. E. Brown, J. Ryburn, D. J. Saul, W. Lawson, "Culturable bacteria in subglacial sediments and ice from two southern hemisphere glaciers," *Microb. Ecol.* **47**, 329–340 (2004).